

# Discrete Assembly of Unmanned Aerial Systems

Christopher G. Cameron<sup>1</sup>, Zach Fredin, and Neil Gershenfeld<sup>2</sup>

**Abstract**—We introduce a modular construction kit for rapidly assembling multi-copter unmanned aerial systems (UAS). The kit consists of voxelized building blocks based on a discrete, face-based decomposition of a cuboctahedral lattice using a circuit board substrate. These voxel building blocks provide the structure of the vehicle, but also create electrical connections for routing power as well as command and control signals. Functional modules including propulsors, power storage, and command and control are designed to interface with the cuboctahedral lattice to create a complete vehicle. We use the system to assemble a 2.6 kg quadcopter UAS in 22 minutes, flight test the resulting vehicle, then disassemble it into components ready for reuse. We examine how the system scales to larger designs, and compare build times and performance with a comparable commercial UAS and equivalent designs built using additive manufacturing.

**Index Terms**—UAS Applications, Modular Robotics, Additive Manufacturing

## I. INTRODUCTION

Unmanned aerial systems (UAS) are rapidly becoming a key component of daily life, with over 800,000 registered in the United States [1]. Nearly half of these are registered for commercial use where they fulfill roles including photography, infrastructure inspection and surveying, and disaster recovery. These numbers will continue to grow as large companies develop heavy-lift applications ranging from UAS package delivery to manned air taxi service. At the same time military applications have grown, with UAS providing key situational awareness data, and development programs investigating opportunities for last-mile resupply to troops in the field.

This range of applications requires small UAS designs covering sizes from less than 250 g to over 25 kg. Users must carefully select their system to meet their requirements for payload and range, while balancing factors such as cost and size. If a user's requirements change, needing a larger payload, or to access a tight space they must make compromises to system performance or invest in a new vehicle. This led US Army Research Laboratory researchers to investigate options to build small UAS on demand to meet a given mission profile and payload. They used additive manufacturing to build quadcopter frames and assembled them using commercial-off-the-shelf (COTS) components such as rotors and batteries [2]. While successful, their work

was limited to small systems and operated on a 24 hour schedule from mission need to finished UAS [3]. Any new mission or change in mission requires another build cycle.

Other studies have explored modular approaches to building and combining small UAS. Li et al. created a system with quadcopters joining mid-flight to create a larger vehicle using rectangular frames and magnets [4]. Each building block in this case is a complete quadcopter UAS with all associated complexity. The distributed flight array, built by Oung et al. features individual ducted fan unit cells which are capable of omnidirectional wheeled locomotion and self-assembly on the ground [5]. Only when four unit cells are joined can the resulting vehicle fly, but each element remains complicated with rotor, power and processing onboard. A more decentralized system, the drone reconfigurable architecture, uses ducted fan propulsor units, with a central control unit along with small connection components [6]. In all cases the systems trade complicated, heavy, and expensive unit building blocks for system capability; a common issue in modular robotics [7].

An alternative approach to customized aerostructure construction has its roots in discretely assembled lattice materials. The first study in this line of research produced a record-setting specific stiffness carbon-fiber lattice structure [8]. The concept has since been extended to creating ultralight morphing aerostructures [9], [10], with compliance tailored through the selective placement of the discrete building blocks. Recently Jennet et. al introduced a unique, face-based decomposition of the cuboctahedral unit cell which enables cheap mass-production of lattice voxels [11]. This design lends itself to automated assembly using small robots [12], and has been used to build reconfigurable, macro-scale mechanical metamaterials and a single-occupant supermileage vehicle. However, these lattice structures require custom, post-hoc actuation, control, and power routing to become fully functional vehicles.

Our study leverages this discretely assembled lattice material framework with a novel voxel design to form the mechanical and electrical backbone of an unmanned aerial system. We extend the work of Jennet to integrate power and data routing with the lattice structure and make the mechanical and electrical connections simultaneously. To complete the system we introduce a library of lattice-compatible accessories including motors, batteries and a flight controller which draw power from and communicate using the lattice bus. These discrete voxel building blocks allow the system to be rapidly assembled, disassembled and reconfigured while keeping the majority of the structure lightweight, stiff and inexpensive. We use these building blocks to assemble a 2.6

Research was funded by the U.S. Army Research Lab under Cooperative Agreement #W911NF1920117, as well as CBA Consortia funding.

<sup>1</sup>Christopher G. Cameron is with the DEVCOM Army Research Laboratory, Aberdeen, MD, United States [christopher.g.cameron.civ@army.mil](mailto:christopher.g.cameron.civ@army.mil)

<sup>2</sup>Zach Fredin and Neil Gershenfel are with the Massachusetts Institute of Technology Center for Bits and Atoms Cambridge, MA, United States

kg quadcopter in 22 minutes, demonstrate low speed flight and hover, and then disassemble the quadcopter back into components ready for reuse. We also compare our discretely assembled quadcopter with additively manufactured alternatives and explore how our system scales to larger vehicle sizes.

## II. DESIGN

The system was originally developed as a concept for a modular, legged robot-material system. A preliminary design exercise suggested that the robotic concept could be adapted into a quadcopter demonstrator with an approximately 2.5kg maximum gross weight and 0.5 kg payload capable of 20-30 minutes flight time. We used these targets as the basis for the detailed designs presented in this section.

### A. Voxel Design

The voxel is the fundamental structural and electrical building block of the UAS. The design uses Jennet's face-based decomposition of the cuboctahedral unit cell to create PCB faces with laminated acetal spacers shown in Figure 1. The FR4 PCB provides the main structural element, while also routing power, ground and a serial communication line to each of the four corners of the voxel face. Six of these faces are then joined together at the corners using mechanical keying and solder joints. For this prototype the solder joints are structural and also connect the six voxel faces electrically. A complete voxel weighs 47 grams with side-length of 102 mm.

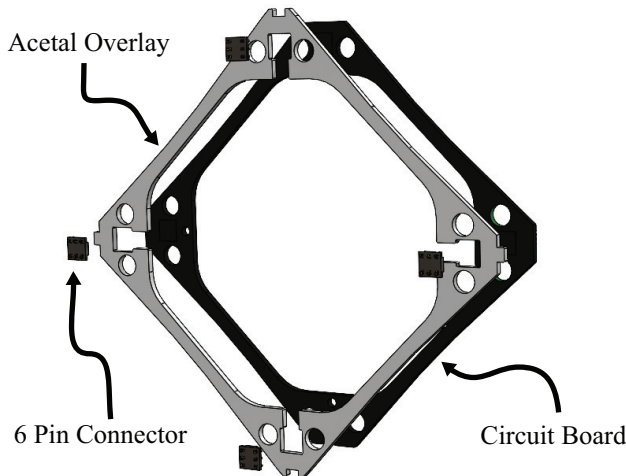


Fig. 1. Exploded view of laminated voxel face

The voxels join face-to-face using the four inter-voxel connections at each corner shown in figure 2. Each corner has a hole sized for a blind rivet which pulls the faces together, while the electrical connections are made using a six position COTS battery spring connector (Molex 0788641001). For flexibility of assembly the electrical connection at each corner is hermaphroditic, with pairs of conductors carrying power, ground and data signals respectively. With four corner

connections, each face-to-face connection has 8 pins per circuit; power, ground and data, enabling redundancy and higher power capacity.

### Soldered Connection

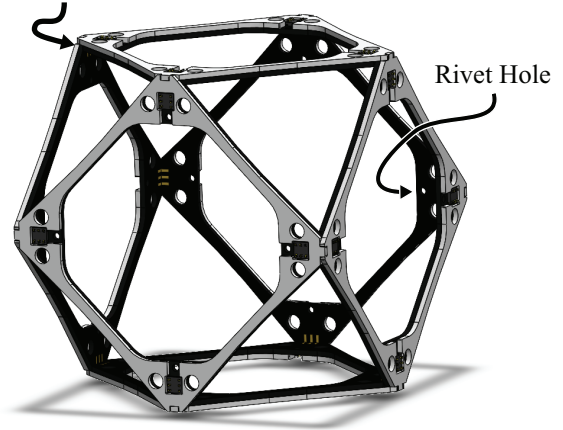


Fig. 2. Fully assembled lattice voxel

1) *Electrical Characterization:* The electrical connectors are rated for 1 Amp continuous current per contact with 30 mOhm contact resistance when mated to properly designed landing pads. With four connectors per face and two pins per circuit we would expect the voxels to be able to transmit 8 Amps of current. However, in our application the connectors in adjacent faces are mated pin-to-pin rather than to a pad. To quantify the effect of this unconventional application, and verify safety limits we ran a series of tests to measure contact resistance and heating in the joints. An Agilent E3633A DC power supply was used to apply constant current across voxels in series and the resulting voltage drop used to calculate resistance as shown in Figure 3 a. Each incremental voxel joint adds  $7\text{ m}\Omega$  of resistance, nearly a factor of two worse than the datasheet value for a properly designed land where we would expect  $3.75\text{ m}\Omega$  incremental resistance. Joint steady state temperature was measured for currents between 1 and 16 Amps as shown in Figure 3 b. Based on the results the voxels can safely transmit 16 Amps of current for periods of time on the order of minutes without exceeding the operating temperature limit of 85 C. This increased power-handling is likely due to the openness of the voxel design enabling greater cooling than accounted for in the datasheet.

### B. Functional Modules

The functional modules transform the lattice from generic structural building blocks into an application specific system. In the case of the discrete UAS the most important functional component is the motor-rotor system shown in figure 4. A key constraint in the design of the motor-rotor system was managing drive current to remain in the limits of the lattice assembly. We selected the T-motor antigravity-4004 300 Kv brushless DC motor with a 15 inch diameter propeller for their high efficiency and low current draw. Manufacturer data indicates that this combination produces a maximum of 1300

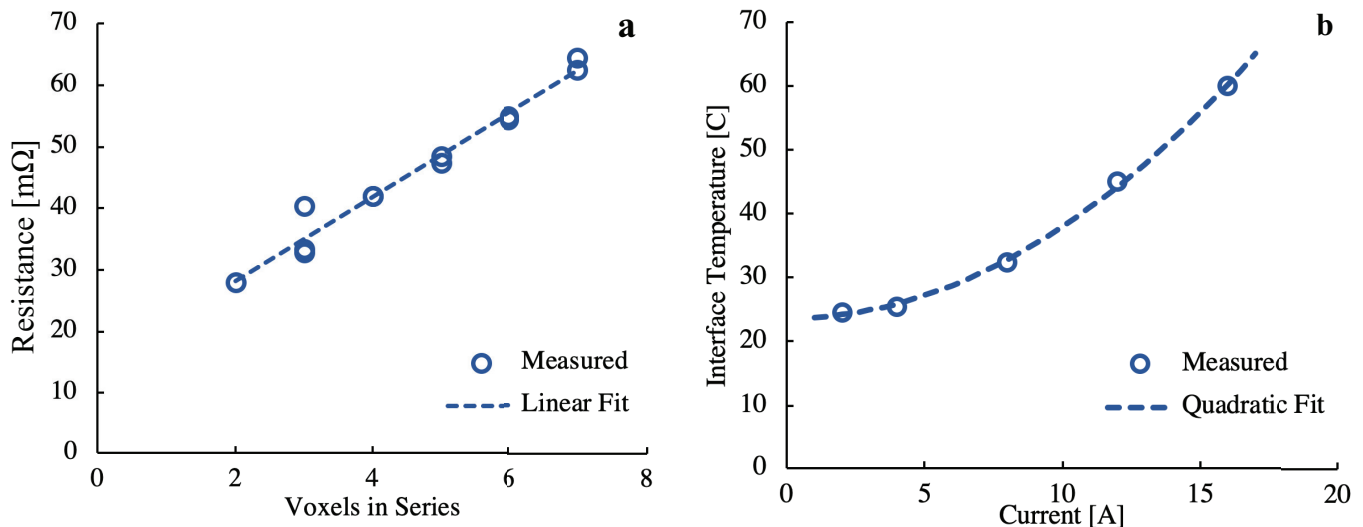


Fig. 3. Results from voxel current testing a) Resistance of voxel assemblies in series b) Temperature rise of voxel connectors with current

grams of thrust at 24 Volts and 8 Amps, just inside the rated current draw of the voxel face connections. The complete motor functional unit combines the motor and rotor with a hardwired T-Motor F35A motor controller on a 3D printed base with a voxel face attachment.

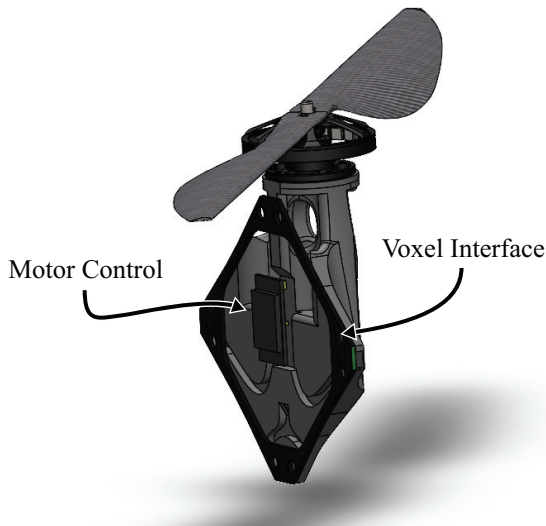


Fig. 4. Motor module incorporating the motor, speed controller and propeller

The energy storage functional units are built around Turnigy 6s 1000 mAh lithium polymer battery packs shown in figure 5. These batteries are enclosed in a 3D printed case with integrated blade-style power connector. The cases are designed to mate with battery holders which remain riveted to the primary voxel structure. The holders secure the batteries with a snap flexure, and incorporate a fast-blow fuse for safety of flight. Various numbers of batteries may be connected in parallel using these holders to trade payload and endurance requirements of the UAS.

The final module is the integrated command and control

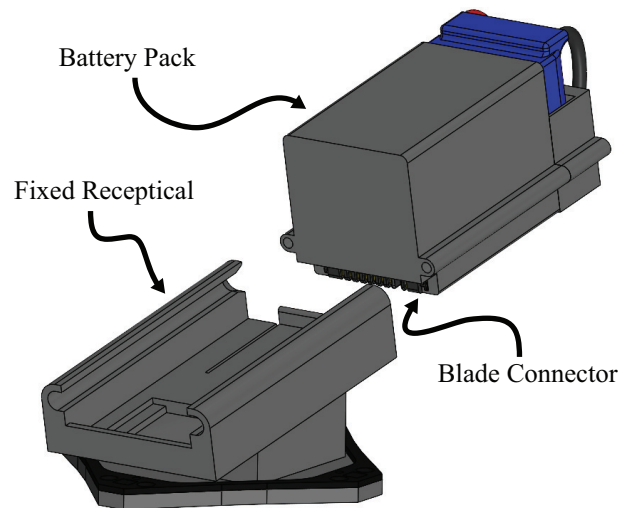


Fig. 5. Battery module with base and removable battery

module shown in figure 6. Flight control and stabilization is implemented on a Teensy 4.0 development board. The software is adapted from the open-source code dRehmFlight VTOL [13] with modifications made to the motor output and inertial measurement unit (IMU) interface routines. An LSM9DS1 9 degree of freedom IMU was used to measure vehicle attitude and a FrsKy XSR 2.4 Ghz radio transceiver used to communicate with the ground station. The system is powered from the common 22 Volt voxelcopter bus with a 5 Volt switch mode step-down transformer. The total power draw of the command and control module is 3 watts.

### III. ASSEMBLY AND FLIGHT TESTING

#### A. Assembly

The complete set of voxels and functional modules is shown in figure 7 a. Final assembly was performed in two

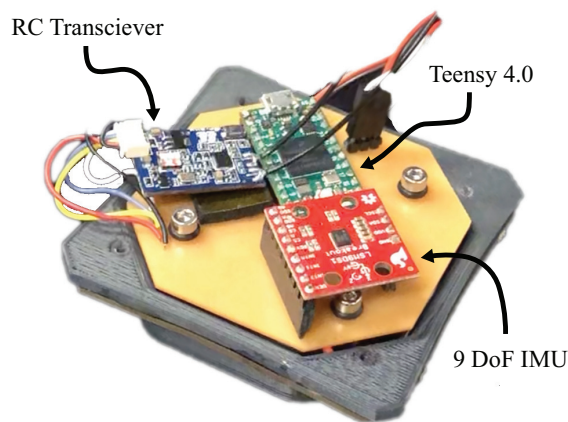


Fig. 6. Command and control module

steps. First the voxels were riveted together forming the complete vehicle frame. 3/16" in diameter blind aluminum rivets were installed using a pneumatic rivet gun. Checks for power and signal continuity were performed with each new voxel riveted in place, and complete frame power handling measurements performed using the benchtop power supply. After these diagnostics the accessory elements were riveted in place and the vehicle checked for electrical issues. The complete assembly time, excluding power-handling measurements, was 22 minutes.

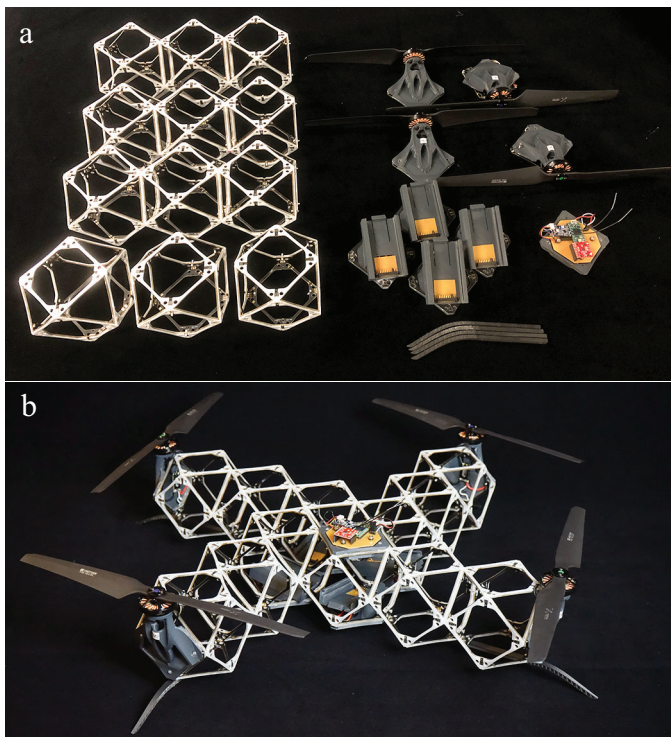


Fig. 7. UAS assembly, a - components prepped for assembly, b - Completed UAS

The assembled vehicle is shown in Figure 7 b. The UAS

measures 660 mm diagonally across motor centers and 1037 mm with rotors attached. The vehicle weighs 2.2 kg with all four batteries installed and the maximum takeoff weight is 2.6 kg, limited by rotor thrust with a 100% margin for maneuverability. Note that the final assembly includes four legs, printed out of a reinforced nylon material, to absorb any hard landings during flight testing. A complete weight breakdown is provided in table I.

TABLE I  
PROTOTYPE UAS WEIGHT BREAKDOWN

Component	Weight [g]	Quantity	Total Weight [g]
Voxel	47	12	564
Rotor	124	4	496
Battery	211	4	844
Battery Base	55	4	220
C2 Module	66	1	62
Legs	6	4	24
Total Vehicle			2210

### B. Flight Test and Comparison to COTS Solution

We conducted flight testing at an indoor track facility on the Massachusetts Institute of Technology Campus. The goal of the testing was to verify that the UAS could enter into a stable hover and maneuver at low speeds, and measure power consumption to estimate hover endurance. We performed a series of short flights totalling 6 minutes. Maneuvering included hover and climb, as well as low speed translation in a 15 by 15 by 3 meter flight zone. The vehicle was stable, with no apparent interference due to noise on the serial bus or issues with power transmission. After flight we measured the expended battery capacity during the recharging cycle as 200 mAh. This represents 22% of the total capacity including a 10% safety margin. The resulting maximum hover endurance is then approximately 27.5 minutes.

TABLE II  
COMPARISON WITH COMMERCIAL UAS

	Discrete Quadcopter	DJI Inspire
Diagonal Dimension	660 mm	605 mm
Propeller Diameter	380 mm	380 mm
Empty Weight	2.21 kg	3.44 kg
Max Takeoff Weight	2.60 kg	4.25 kg
Payload	0.40 kg	0.81 kg
Battery	6s 4000mAh	6s 8560 mAh
Hover Endurance	27.5 min	27 min <sup>1</sup>

<sup>1</sup> With 275 g payload

Table II shows a comparison of the discretely assembled quadcopter parameters with those of a similar COTS UAS, the DJI Inspire 2 provided in the operating manual [14]. Both vehicles have 15 inch diameter rotors and a similar ground footprint, and both can hover for nearly half and hour. However, the Inspire 2 is 60% heavier and capable of carrying twice the payload of the discrete quadcopter. This is largely due to the conservative motor sizing dictated by the data sheet rated current of the lattice connectors.

#### IV. SCALING AND COMPARISON TO ADDITIVE MANUFACTURING

A key advantage of this system is the modularity may be leveraged to build many different vehicles. Figure 8 shows the payload-endurance curves for three vehicles; the quadcopter test flown as part of this study, as well as notional designs for larger hexacopter and octocopters. The quadcopter and hexacopter designs carry 4 battery modules, while the octocopter includes 6. Increasing the number of rotors to six and eight significantly increases payload capacity to 1 and 1.6 kg respectively at the expense of larger vehicle footprint. The increase in maximum payload capacity also comes with a decrease in hover endurance for a given payload. The quadcopter at maximum payload of 0.4 kg has a hover endurance of 22 minutes, while the hexacopter and octocopter achieve only 19.5 and 17.5 minutes respectively. While none of these systems matches the absolute performance of the DJI Inspire 2 from Table II, as a whole, they are capable of a wider range of missions. For example, a single octocopter used for a heavy payload delivery may be disassembled into two quadcopters for carrying out longer endurance surveillance missions with lighter payloads.

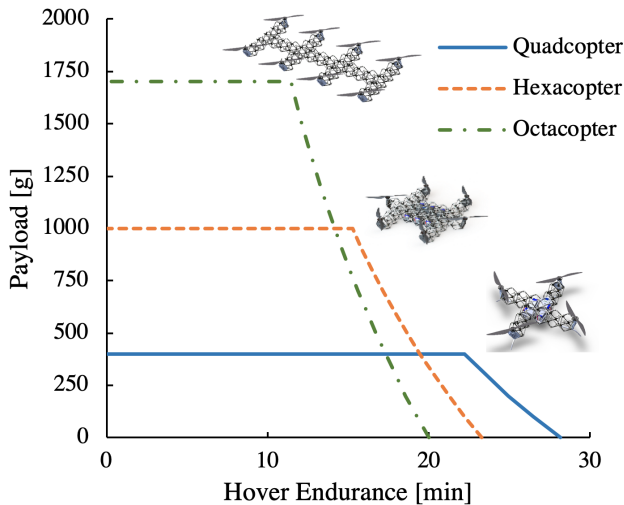


Fig. 8. Payload-endurance curves for three discrete UAS designs

Properly designed discretely assembled structures can surpass the material throughput and build volume of traditional additive manufacturing techniques [11]. In the case of the discrete quadcopter we compare our to a vehicle with the same functional components, but with a frame printed on commercial fused deposition modeling (FDM) systems. A rendering of this notional FDM quadcopter frame is shown in Figure 9 a. The design consists of a central body with four arms, including integrated motor mounts. The arms were designed with a circular cross section and 2mm wall thickness. The diameter was chosen to match the calculated bending stiffness of the voxelcopter arms by rearranging the expression for cross-sectional stiffness of an annular ring with radius  $r$  and thickness  $t$ :

$$EI_{voxel} = E_{fdm} \frac{\pi}{4} (r^4 - (r-t)^4) \quad (1)$$

$$EI_{voxel} \approx E_{fdm} \pi r^3 t \quad (2)$$

$$t = \frac{EI_{voxel}}{E_{fdm} \pi r^3} \quad (3)$$

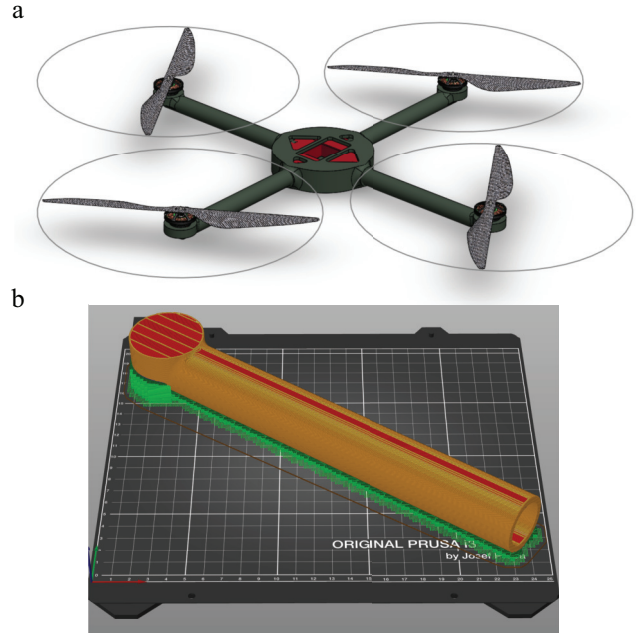


Fig. 9. Additively manufactured UAS alternative a) Frame rendering b) Arm post-processed for manufacturing with FDM 3D printer

Results in table III are presented for frames using both a Prusa Mark 3 consumer grade printer with PLA filament [15], as well as a Markforged X7 enterprise machine with their Onyx short-fiber reinforced nylon material [16]. Print times are calculated using Prusa Slicer and Markforged eiger toolpathing programs, with an example toolpath shown in Figure 9 b. The largest default layer heights of 0.3 mm and 0.2 mm are used and supports are included everywhere. Each arm takes 6 to 9 hours to print depending on the printer, while the main body takes 10 hours on the Prusa and nearly 20 hours using the Markforged system. The minimum print time is then 16-20 hours with at least 3 printers working in parallel. The final vehicle assembly time will be several hours longer given post-processing and bonding, as well as wiring and soldering of electronics. By comparison, assembly of the discrete quadcopter took only 22 minutes, with post-flight disassembly taking slightly longer at 24 minutes. Additionally, there is no post-assembly wiring or soldering necessary with the discrete system. As a tradeoff, the 3D printed frames are lighter than the discretely assembled frame, and would result in a 50-60% increase in payload capacity or a 14-17% increase in hover endurance compared to our discrete quadcopter design.

TABLE III  
ADDITIVELY MANUFACTURED UAS FRAMES

	Prusa i3 Mk3s+	Markforged X7
Modulus of Elasticity	2.0 GPa	2.4 GPa
Arm Diameter	26 mm	24 mm
Arm Print Time	6h 29m	9h 40m
Body Print Time	10h 30m	19h 4m
Frame Weight	364 g	343 g

## V. CONCLUSIONS AND FUTURE WORK

We designed and built a modular construction system for small UAS. The system uses functional units including power, motors, and controllers, to interface with an underlying mechanical and electrical lattice built using discrete voxel building blocks. The prototype system was built using laminated pcb fabrication and readily available compression connectors, with additively manufactured functional units. We used the prototype system to build a 2.6 kg quadcopter UAS in 22 minutes, an order of magnitude faster than equivalent systems built using FDM additive manufacturing. Flight testing demonstrated vehicle controllability and an estimated hover endurance of 27 minutes, comparable to a similarly sized commercial system. The flexibility of the discrete system does come with compromises in performance. A state of the art commercial UAS of similar overall dimensions carries twice the payload of the discrete system with similar hover endurance, largely due to current carrying limitations of the prototype lattice. After flight testing, the riveted joints were disassembled into the original components ready to build additional systems.

This first study demonstrates the feasibility of the discrete UAS concept and opens the door for follow-on investigations to improve flight performance and overall system capability:

- Adopt reel-to-reel Molex ASEP [17] insert-moulded technologies for mass production of voxel faces with higher power handling and elimination of soldered joints
- Significantly increase flight time by switching to high energy density lithium ion battery chemistry without sacrificing performance due to the low current system design
- Characterize of system download, drag and forward flight performance
- Automate system reconfiguration using modular robotics toolkit developed for manipulating voxel building blocks
- Explore variation of propulsor size and orientation

Along with these improvements, work is necessary to incorporate automated discovery of control laws for different UAS topologies. This effort could extend to a redesign of the underlying voxels to enable the UAS to map its own topology after construction or reconfiguration.

## ACKNOWLEDGMENT

The authors would like to thank MIT's Department of Athletics, Physical Education and Recreation for providing

the indoor track facility for flight testing, as well as Molex Corporation for collaboration on future designs. Special thanks to Alfonso Parra Rubio for assisting with flight testing and videography of the discretely assembled quadcopter.

## REFERENCES

- [1] FAA, "Uas by the numbers." [Online]. Available: [https://www.faa.gov/uas/resources/by\\_the\\_numbers/](https://www.faa.gov/uas/resources/by_the_numbers/)
- [2] P. Mangum, Z. Fisher, K. D. Cooksey, D. Mavris, E. Spero, and J. W. Gerdes, "An automated approach to the design of small aerial systems using rapid manufacturing," in *Volume 2B: 41st Design Automation Conference*. Boston, Massachusetts, USA: American Society of Mechanical Engineers, Aug. 2015.
- [3] "Army engineers demonstrate new system for on-demand 3-D printed drones." [Online]. Available: [https://www.army.mil/article/180189/army\\_engineers\\_demonstrate\\_new\\_system\\_for\\_on\\_demand\\_3\\_d\\_printed\\_drones](https://www.army.mil/article/180189/army_engineers_demonstrate_new_system_for_on_demand_3_d_printed_drones)
- [4] G. Li, B. Gabrich, D. Saldaña, J. Das, V. Kumar, and M. Yim, "ModQuad-Vi: A Vision-Based Self-Assembling Modular Quadrotor," in *2019 International Conference on Robotics and Automation (ICRA)*, May 2019, pp. 346–352, iSSN: 2577-087X.
- [5] R. Oung, F. Bourgault, M. Donovan, and R. D'Andrea, "The Distributed Flight Array," in *2010 IEEE International Conference on Robotics and Automation*, May 2010, pp. 601–607, iSSN: 1050-4729.
- [6] M. A. da Silva Ferreira, M. F. T. Begazo, G. C. Lopes, A. F. de Oliveira, E. L. Colombini, and A. da Silva Simões, "Drone Reconfigurable Architecture (DRA): a Multipurpose Modular Architecture for Unmanned Aerial Vehicles (UAVs)," *Journal of Intelligent & Robotic Systems*, vol. 99, no. 3-4, pp. 517–534, Sep. 2020. [Online]. Available: <https://link.springer.com/10.1007/s10846-019-01129-4>
- [7] M. Yim, W.-m. Shen, B. Salemi, D. Rus, M. Moll, H. Lipson, E. Klavins, and G. S. Chirikjian, "Modular Self-Reconfigurable Robot Systems [Grand Challenges of Robotics]," *IEEE Robotics Automation Magazine*, vol. 14, no. 1, pp. 43–52, Mar. 2007, conference Name: IEEE Robotics Automation Magazine.
- [8] K. C. Cheung and N. Gershenfeld, "Reversibly Assembled Cellular Composite Materials," *Science*, vol. 341, no. 6151, pp. 1219–1221, Sep. 2013. [Online]. Available: <http://www.sciencemag.org/cgi/doi/10.1126/science.1240889>
- [9] B. Jenett, S. Calisch, D. Cellucci, N. Cramer, N. Gershenfeld, S. Swei, and K. C. Cheung, "Digital morphing wing: Active wing shaping concept using composite lattice-based cellular structures," *Soft Robotics*, vol. 4, no. 1, pp. 33–48, Mar. 2017. [Online]. Available: <https://www.liebertpub.com/doi/10.1089/soro.2016.0032>
- [10] N. B. Cramer, D. W. Cellucci, O. B. Formoso, C. E. Gregg, B. E. Jenett, J. H. Kim, M. Lendraitis, S. S. Swei, G. T. Trinh, K. V. Trinh, and K. C. Cheung, "Elastic shape morphing of ultralight structures by programmable assembly," *Smart Materials and Structures*, vol. 28, no. 5, p. 055006, May 2019. [Online]. Available: <http://stacks.iop.org/0964-1726/28/i=5/a=055006?key=crossref.70db3e3ae1cc81050605038c3bdde724>
- [11] B. Jenett, C. Cameron, F. Tourlomis, A. P. Rubio, M. Ochalek, and N. Gershenfeld, "Discretely assembled mechanical metamaterials," *Science Advances*, vol. 6, no. 47, p. eabc9943, 2020. [Online]. Available: <https://www.science.org/doi/abs/10.1126/sciadv.abc9943>
- [12] B. Jenett, A. Abdel-Rahman, K. Cheung, and N. Gershenfeld, "Material-robot system for assembly of discrete cellular structures," *IEEE Robotics and Automation Letters*, vol. 4, no. 4, pp. 4019–4026, 2019.
- [13] D. Rehm, "dRehmFlight VTOL: Teensy flight controller and stabilization," Jul. 2019. [Online]. Available: <https://github.com/nickrehm/dRehmFlight>
- [14] DJI, "Inspire 2 Series User Manual," Jul. 2019. [Online]. Available: <https://www.dji.com/downloads/products/inspire-2>
- [15] Prusa, "Prusament PLA by Prusa Polymers," Sep. 2018. [Online]. Available: <https://prusament.com/materials/pla/>
- [16] Markforged, "Material Datasheet Composites," Jan. 2022. [Online]. Available: <https://www-objects.markforged.com/craft/materials/CompositesV5.2.pdf>
- [17] Molex, "Asep solutions," Jul. 2019. [Online]. Available: <https://www.content.molex.com/dxdam/literature/987651-7641.pdf>